A New Genetic Method for Subpixel Mapping Using Hyperspectral Images

Xiaohua Tong, Xiong Xu, Antonio Plaza, *Fellow, IEEE*, Huan Xie, Haiyan Pan, Wen Cao, and Dong Lv

***Abstract*—Subpixel mapping techniques aim to obtain the spatial location and distribution of subpixels by transforming the information coming from a set of input abundance maps into a classification result with higher spatial resolution. However, traditional subpixel mapping algorithms generally ignore the possible errors that are due to abundance estimation inaccuracies by spectral unmixing techniques. In this paper, we propose a new genetic algorithm-based subpixel mapping technique that solves the subpixel mapping problem by correcting the potential errors in the estimated abundance fractions used as input to the subpixel mapping process. The proposed algorithm has been compared with other two genetic subpixel mapping methods, using both synthetic and real hyperspectral images. Our experimental results demonstrate that the proposed approach outperforms traditional subpixel mapping algorithms, thus providing an effective option to improve the accuracy of subpixel mapping for remotely sensed hyperspectral images.**

***Index Terms*—Genetic algorithms, hyperspectral imaging, spectral unmixing, subpixel mapping.**

I. Introduction

THE SIGNAL recorded by a hyperspectral sensor is generally a mixture of the reflected radiation scattered by the underlying constituent substances located in a given pixel [1]. Spectral unmixing techniques focus on discriminating different materials in mixed pixels and obtaining the corresponding fractions of the so-called endmembers (pure spectral components). However, the spatial distribution of the endmembers in the pixel cannot be inferred from the estimated endmember abundance maps. For this reason, subpixel mapping (or super-resolution mapping) has been introduced to solve this problem by dividing a pixel into subpixels and assigning each subpixel to a land-cover class, in order to convert the abundance map to a hard classification map with higher spatial resolution [2].

Subpixel mapping is an ill-posed problem that attempts to obtain a finer classification map from a coarser abundance image. To tackle this problem, several subpixel mapping methods have been proposed based on the concept of spatial dependence [3]–[31], which refers to the property that pixels which are spatially adjacent in the scene are more likely to be similar than those that appear in spatially disjoint areas. As a typical inverse problem [3], artificial intelligence algorithms have been widely used to automatically label subpixels using spatial dependence properties owing to their global optimization abilities [4]–[14]. For instance, artificial neural networks (ANNs), as powerful tools for nonlinear prediction, have been applied to subpixel mapping by constructing the projection relationship between the abundance map and the subpixel mapping output [4]–[7]. To deal with different types of mixed pixels, Xu *et al.* [8] designed a multiagent system algorithm to reconstruct possible features during the subpixel mapping procedure. Furthermore, based on the spatial dependence criterion, several objective functions were established and different optimization techniques were utilized in previous works [9]–[16]. Given a certain objective function, genetic algorithms aim at generating the final result by incorporating different operators [9]. Besides, Villa *et al.* [10] utilized a simulated annealing technique to finalize the subpixel mapping procedure with another different objective function. Based on the objective function proposed in [11], Zhong *et al.* adopted differential evolution [12] and artificial immune system techniques [13] to perform optimization in the context of subpixel mapping, respectively. Moreover, A particle swarm optimization algorithm was used in [14] as a postprocessing on a previously derived subpixel mapping result.

Genetic algorithms have been widely used in various fields and proved to be simple but efficient global optimization methods [32]–[35]. These kinds of techniques can be used to search for an optimal solution without trying all possible cases [36]–[37]. Inspired by the principle of "survival of the fittest" in natural evolution processes, the basic idea of the method is that different operators collaborate to generate the optimal solution iteratively for a population of individuals that represent possible solutions. For example, the selection operator aims to pass on genes of better individuals to the next generation; the crossover and the mutation operators can effectively avoid converging to local optima and thus better search for an optimal solution [38]. When it comes to the subpixel mapping problem,

Manuscript received June 10, 2015; revised September 15, 2015; accepted October 26, 2015. Date of publication March 02, 2016; date of current version September 30, 2016. This work was supported in part by China Postdoctoral Science Foundation (Project nos. 2014M560353, 2015T80450), in part by the National Natural Science Foundation of China (Project no. 41401398, 41325005, 41201426, 41171352, and 41171327), in part by the Fund of Shanghai Outstanding Academic Leaders Program (Project No. 12XD1404900), and in part by Kwang-Hua Foundation of College of Civil Engineering, Tongji University. *(Corresponding author: Xiaohua Tong.)*

X. Tong, H. Xie, H. Pan, W. Cao, and D. Lv are with the College of Surveying and Geo-Informatics, Tongji University, Shanghai 200092, China (e-mail: xhtong@tongji.edu.cn; huanxie@tongji.edu.cn; hypan@tongji.edu.cn; caowenrs@126.com; 1134601@tongji.edu.cn).

X. Xu is with the College of Surveying and Geo-Informatics, Tongji University, Shanghai 200092, China, and also with the Hyperspectral Computing Laboratory, Department of Technology of Computers and Communications, Escuela Politecnica, University of Exremadura, 10003 Cáceres, Spain (e-mail: xvxiong@tongji.edu.cn).

A. Plaza is with Hyperspectral Computing Laboratory, Department of Technology of Computers and Communications, Escuela Politecnica, University of Exremadura, 10003 Cáceres, Spain (e-mail: aplaza@unex.es).

Color versions of one or more of the figures in this paper are available online at http://ieeexplore.ieee.org.

Digital Object Identifier 10.1109/JSTARS.2015.2496660

different combinations of operators and objective (or fitness) functions have been designed [9], [30], [31]. In addition to the selection and crossover operators, Mertens *et al.* [10] devised an inversion operator that is used to invert the order of the genes of an individual. Zhao *et al.* [30] utilized the traditional selection operator and a specifically defined crossover operator to generate the final subpixel mapping result. Moreover, genetic algorithm-based subpixel mapping has also been applied for wetland inundation estimation [31].

However, an important aspect of genetic-based subpixel mapping methods is that they generally rely on the estimated abundance map as a baseline, which means that the proportions of different classes in mixed pixels will remain unchanged during the process of subpixel mapping, and crossover operators are commonly designed under this circumstance to generate the final subpixel mapping output without bearing in mind the potential errors that could be introduced by spectral unmixing techniques [39]. Although linear spectral unmixing techniques have shown their effectiveness in decomposing mixed pixels [40], in many situations, the estimated abundances may not be completely accurate due to noise, atmospheric interferers, nonlinearity of the mixtures, and so on. As a result, potential inaccuracies in abundance estimation may introduce significant errors in the subpixel mapping process and the resulting thematic maps.

This inspired us to propose, as a novel contribution of this work, the use of a mutation operator, and therefore, a new subpixel mapping method based on genetic algorithms which corrects potential abundance inaccuracies to obtain the final solution. With the introduced mutation operator, which alters the gene value randomly, the proportions of classes in mixed pixel can be adjusted to search for a better result. Although the mutation operator can alter the inaccuracies in abundance maps, the subpixel mapping result may suffer from excessive distortion due to the fact that only spatial dependence is utilized in the fitness function and the ability of the mutation operator is hard to confine. Therefore, a weighted spectral term was also formulated and incorporated into the fitness function so that the impact of the original spectral information can still be taken into consideration to avoid excessive mutations.

In conclusion, the proposed genetic method considers subpixel mapping as an optimization problem which maximizes spatial dependence (by establishing subpixel associations that promote the grouping of pixels which are spatially adjacent in the scene) and minimizes the possibly negative impact of abundance estimation inaccuracies by allowing the genetic algorithm to modify the gene value of individuals, in which case, the utilized abundance map can be modified indirectly. In this way, the proposed method is expected to achieve a better solution when compared with traditional genetic subpixel mapping methods.

The remainder of this paper is organized as follows. Section II gives a detailed description of the proposed method. Section III presents experimental results obtained using both synthetic and real hyperspectral scenes. Section IV concludes the paper with some remarks and hints at plausible future research lines.

II. Proposed Subpixel Mapping Method

The key issue in a subpixel mapping problem is how to determine an optimal subpixel distribution of each class within a pixel. Inspired from Tobler's first law [41], [42], spatial dependence has been regarded as a relevant criterion. It simply refers to the tendency of spatially close observations to be more alike than more distant observations [2]. As illustrated in Fig. 1, given an abundance map obtained by spectral unmixing techniques, each coarse pixel can be divided into $\mathrm{S} \times \mathrm{S}$ subpixels, where S represents the scale factor. The number of subpixels for each land-cover class can be determined by the fractional values of different classes. Fig. 1 shows a subpixel mapping example with three classes. As shown in Fig. 1(a), a coarse pixel is divided into 16 (4×4) subpixels, where the scale factor S equals 4, and 0.5 in the fraction image in red, which means that 8 (16×0.5) subpixels belong to land-cover class 1. Fig. 1(b) and (c) describes two possible distributions of subpixels. Given the principle of spatial dependence, the latter is perceived to be less optimal.

As mentioned before, for traditional genetic-based subpixel mapping methods, the spatial dependence is considered as the sole criterion for defining the fitness function, and the constraint on abundance fractions is strictly satisfied (meaning that the initial estimation of abundance fractions will have a great impact on the final subpixel mapping result). The main innovation of our proposed method is that possible inaccuracies and errors in abundance estimation are taken into consideration and the mutation operator is utilized to adjust the abundance fractions by modifying the attribution values of subpixels. Specially, a weighted spectral term is incorporated into the fitness function to avoid the severe discrepancy between the generated subpixel mapping result and the original hyperspectral imagery. In the following, we provide a description of our proposed approach.

Fig. 2 shows a general flow of the proposed method, which can be summarized by the following steps:

1) First, an abundance map is obtained from the original hyperspectral scene using a spectral unmixing technique. For each pixel in the abundance map, an initial population of solutions is generated randomly. Each individual of the population is a solution of a possible configuration of different endmembers for a given mixed pixel.
2) At this point, three different kinds of operators, i.e., selection, crossover, and mutation are used to increase the fitness of the whole population after iterating (while removing some individuals that did not exhibit a good overall fit).
3) Finally, the individual with the best overall fit is identified and retained as the one providing the optimal configuration for a given pixel, after all iterations have been completed.

Let us denote the original hyperspectral image by $\mathbf{y}$. This image contains K bands and m pixels, and we use y_i^k to denote the kth band of pixel i. Let us also suppose that the spectral unmixing model yields a set of abundance fraction maps $\mathbf{x}$ for C endmembers, so that each mixed pixel in the original scene can be divided into $S \times S$ subpixels, assuming that S

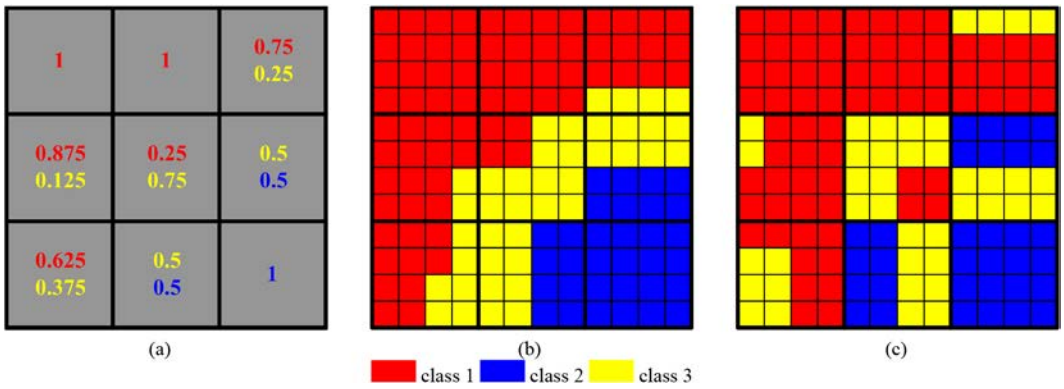

Fig. 1. Toy example illustrating subpixel mapping methods. (a) Abundance maps are extracted for a 3×3 -pixel image. (b) A possible distribution of subpixels in a finer resolution image in which a coarse pixel is divided into 16 (4×4) subpixels. (c) Another distribution which is perceived as less optimal than the one reported in (b).

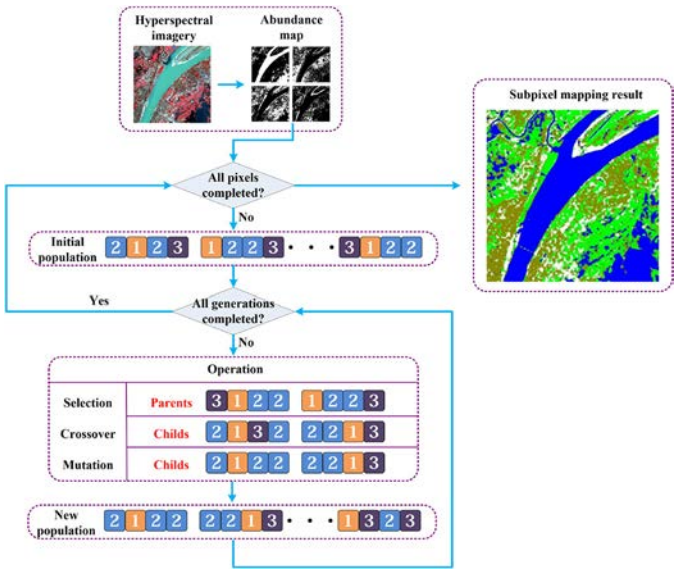

Fig. 2. Framework of the proposed method.

is the scale factor. With the aforementioned notations in mind, the number of subpixels to be assigned to the class given by endmember c in the mixed pixel i can be calculated as follows:

$$NS_i^c = \text{round}(x_i^c \times S \times S) \tag{1}$$

where x_i^c is the abundance fraction of class c in pixel i, and *round()* is an operator to convert the input to the nearest integer. Then, the initial population of solutions for each mixed pixel i can be generated randomly under a constraint given by the calculated NS_i^c, $c \in [1, C]$. Specifically, this subpixel number constraint is fulfilled strictly in other genetic subpixel mapping methods [9], [30]. Therefore, the widely used mutation operator was generally discarded. However, since our goal is to correct possible abundance estimation inaccuracies, mutation is the best choice for an operator able to adjust these possible errors by altering each gene (subpixel) value to an arbitrary class label with a certain probability. Therefore, three operators (selection, crossover, and mutation) are utilized in our proposed method. Moreover, in order to restrain the abrupt changes often brought by the mutation operator, a weighted spectral term was integrated with the commonly used spatial dependence term for the considered fitness function.

A. Selection, Crossover, and Mutation Operators

Given an initial population of solutions generated randomly, three kinds of operators are utilized to obtain a new generation. The selection operator aims at retaining the individuals with higher fitness by selecting two individuals as the parents. In this paper, the roulette wheel method was utilized to select the parents according to a probability that is proportional to the fitness, which means that the better the individuals, the more chances they have to be selected.

Once the two parent individuals have been selected, the crossover operator is used. This crossover operator allows for exchanging the genes between two individuals with a certain probability P_c. This operator has the ability to approach the globally optimal solution. In this paper, the one-point crossover method is used for this purpose, and the operator is designed as illustrated in Fig. 3. Specifically, an insert position is first generated randomly, and the latter parts of the two individuals will then perform an exchange of information with each other in order to generate two new individuals.

An important consideration at this point is that the crossover operation should not break the inherent abundance constraint from the parent individuals, and the number of subpixels for different classes should be kept constant between the parent individuals and the generated child individuals. Therefore, after the crossover operation, the two new child individuals have to be adjusted to satisfy the constraint. Our strategy to address this issue is to first assess the differences between parent and child individuals and then exchange class labels of genes until the disagreement is eliminated, as shown in Fig. 4. As a result, two new child individuals are obtained for the new generation.

As mentioned above, the crossover operator aims to approach the global optimization problem under the effective adjustment of the abundance constraint. However, when the abundances are taken into consideration, a mutation operator is utilized in

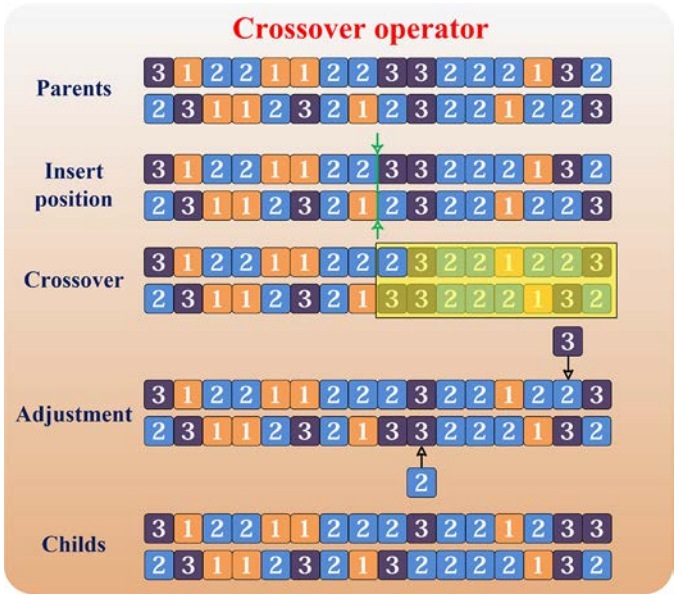

Fig. 3. Example of the crossover operator.

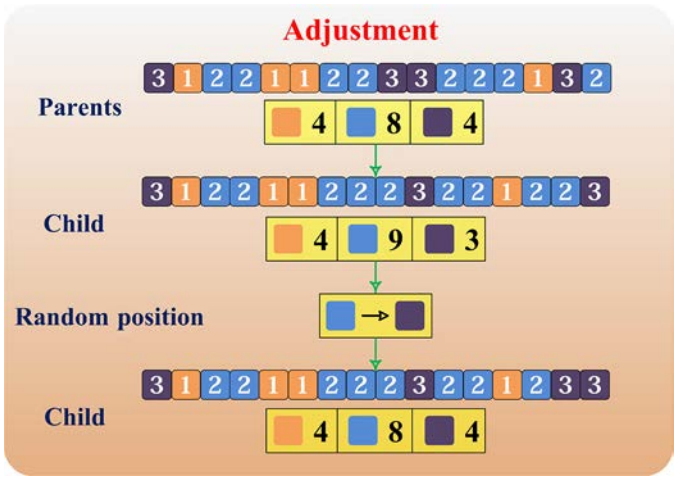

Fig. 4. Illustration of the adjustment process.

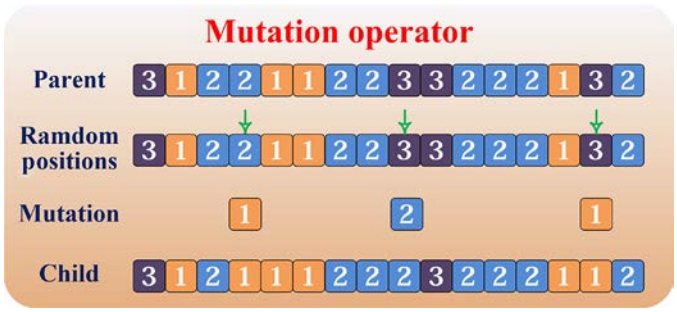

Fig. 5. Example of the mutation operator.

the proposed method. This operator changes a gene from one class to another with a certain probability P_m. By this way, the initial abundance fractions may be modified. Fig. 5 illustrates the implementation of the mutation operator in our proposed approach. As shown in Fig. 5, each gene in the parent individual has a chance to change to other class randomly, so that the child individual can be then obtained. By this way, the proposed method has the ability to modify the previously defined abundance fractions and try to find a better solution given the fitness function, thus correcting potential errors in the initial fractional abundance estimations that serve as the starting condition for the method.

B. Fitness Function

After introducing the three different operators that the genetic algorithm exploits, we focus now on the fitness function as a key aspect to improve the performance of the proposed method. Generally, the spatial dependence principle is formulated as the only criterion to control the search for a global solution. However, a main innovation of our work is that the mutation operator is utilized to correct the possible abundance estimation errors. Accordingly, the effect of the mutation operator should be refined to avoid excessive distortion and ensure the coincidence between the generated subpixel mapping result and the information contained in the original hyperspectral image. To address this issue, we incorporate a weighted spectral term (together with the spatial dependence term) in the fitness function of the proposed method.

Specifically, we use a metric called spatial dependence index (SDI) proposed in [11]. Let j denote a gene (subpixel) in each individual (solution) that corresponds to the original mixed pixel i. The SDI of subpixel j for endmember class c can be calculated as follows:

$$SDI_j^c = \sum_{t \in N[i]} w_{j,t} \times x_t^c \tag{2}$$

where $N[i]$ denotes the set of neighboring pixels of pixel i; $w_{j,t}$ is the weight of neighboring pixel t to subpixel j; and x_t^c is the abundance fraction of pixel t for class c. $w_{j,t}$ is often calculated as the inverse of the distance of the subpixel to the corresponding pixel center [2].

The fitness function based on spatial dependence for all subpixels of each individual can be formulated as

$$\text{Fitness(SD)} = \sum_{j=1}^{S \times S} \sum_{c=1}^{C} v_{j,c} \times SDI_j^c \tag{3}$$

where $v_{j,c}$ is used to model if subpixel j belongs to endmember class c as follows:

$$v_{j,c} = \begin{cases} 1, & \text{if subpixel } j \text{ belongs to class } c \\ 0, & \text{otherwise.} \end{cases} \tag{4}$$

The greater the SDI, the better the individual. In order to ensure spectral consistency, we employed the difference between the original spectral signature $\mathbf{y}_i$ and the inverse (estimated) spectral signature of the same mixed pixel i [which is also known as the root-mean-square error (RMSE)] as follows:

$$\text{Fitness(AI)} = \sqrt{\frac{\|\mathbf{y}_i - \hat{\mathbf{y}}_i\|_2^2}{K}} \tag{5}$$

TABLE I
COMPARISON OF DIFFERENT GENETIC SUBPIXEL MAPPING ALGORITHMS (THE SYMBOL * DENOTES A MODIFIED CROSSOVER OPERATOR WHICH WAS INTRODUCED IN [30])

Methods	Fitness function	Operator			
		Selection	Crossover	Inversion	Mutation
GA	$\sum_{j=1}^{S*S} \sum_{p \in N_s[j]} \frac{\delta_{j,p}}{N_s}$	√	√	√	
MGA	Fitness (SD)	√	√*		
Proposed (GAAI)	Fitness (GAAI)	√	√		√

where $\hat{\mathbf{y}}_i$ is the inverse signature of pixel i, generated from the configuration of each individual. The smaller the difference between the original and the inverse spectral signature, the better the individual.

With these ideas in mind, the fitness function for the proposed method, hereinafter called genetic algorithm able to correct abundance inaccuracies (GAAI), can be formulated as follows:

$$\begin{aligned}\text{Fitness(GAAI)} &= \text{Fitness(SD)} - \lambda \times \text{Fitness(AI)} \\ &= \sum_{j=1}^{S\times S} \sum_{c=1}^{C} v_{j,c} \left(\sum_{t \in N[i]} w_{j,t} \times x_t^c \right) \\ &\quad - \lambda \sqrt{\frac{\|\mathbf{y}_i - \hat{\mathbf{y}}_i\|_2^2}{K}} \end{aligned} \tag{6}$$

where λ is a weight that controls the tradeoff between the spatial dependence and the spectral term.

C. Comparison With Genetic Algorithms-Based Methods

As mentioned before, there are other genetic subpixel mapping algorithms that have been developed in the literature. In this section, we provide a brief comparison of the main properties of our proposed GAAI method with regards to these methods. Specifically, we consider the genetic algorithm (GA) in [9] and the modified genetic algorithm (MGA) in [30]. A comparison of the two algorithms with the proposed method is given in Table I.

In Table I, $N_s[j]$ denotes the set of neighboring subpixels of subpixel j, and N_s is the total number of neighboring subpixels. $\delta_{j,p}$ is used to describe if neighboring subpixel p belongs to the same class as subpixel j

$$\delta_{j,p} = \begin{cases} 1, & \text{if } p \text{ belongs to the same class with } j \\ 0, & \text{otherwise.} \end{cases} \tag{7}$$

From the comparison presented in Table I, we can see that the utilization of the mutation operator and the inclusion of a spectral term in the fitness function are the most relevant innovations of the proposed method with regards to other techniques. An experimental evaluation of the effectiveness of the proposed method will be discussed in the following section.

III. EXPERIMENTS AND ANALYSIS

In our experimental evaluation, the proposed GAAI method was compared with three different subpixel mapping algorithms: the spatial attraction (SA) model in [15], the GA in [9], and the MGA in [30]. In our experiments, we use both synthetic and real hyperspectral images. Specifically, the parameters used for the different genetic algorithms were set empirically and made equal in all tests. More specifically, the size of the population was set to 200; the number of generations was set to 100, and the crossover probability P_c was set to 0.5. Moreover, the mutation probability P_m was set to 0.05 for the proposed method. Moreover, to ensure the convergence of the proposed method, we let the iterative process continue until the result remains unchanged, even the predefined number of iterations has been completed. Owing to the fact that the number of endmembers in a mixed pixel are proportional to the obtained abundance fractions, and due to the need to impose the sum-to-one constraint on the estimated abundances in order to have meaningful subpixel estimates, we have used the fully constraint least squares (FCLS) [43] method to estimate the abundance maps in this work. The accuracy assessment was undertaken using the classification overall accuracy (OA), average accuracy (AA), individual classification accuracies, and the Kappa coefficient of the subpixel mapping result [44]. At the same time, the abundance map can also be generated from the final subpixel mapping result and the RMSE is utilized in this case to compare the reference abundance fractions with the reference classification map.

A. Synthetic Experiments

Two synthetic hyperspectral images have been constructed to test the performance of the proposed GAAI method. In our experiments, the low-resolution hyperspectral image is generated by degrading the available high-resolution hyperspectral image with an averaging filter. In this way, the classification result obtained for the high-resolution image can be used as the ground truth to evaluate different subpixel mapping results.

1) Synthetic Image 1—HJ-1A: To simulate a real world situation under a fully controlled scenario, we used a real hyperspectral data set which was obtained by a Chinese environmental satellite, HJ-1A [45]. The HJ-1A satellite has a hyperspectral sensor with 115 spectral bands (in the spectral range from 0.45 to $0.95\,\mu\text{m}$) and spatial resolution of 100 m per pixel. The utilized HJ-1A image (150×150 pixels) was acquired on August 19, 2009, and was used as the original image in our experiments. The study site is located in Hanchuan City, Hubei Province, central China, and its surrounding area. Four land-cover classes, i.e., urban, agricultural land, water, and vegetation are used to characterize this image as shown in Fig. 6(b). This image was degraded artificially to obtain a low-resolution synthetic image given a scale factor of three in this experiment.

As illustrated in Fig. 6, the abundance map used as initial condition can severely impact the final subpixel mapping results. Compared with the reference classification map in Fig. 6(b), obtained using the support vector machine (SVM)

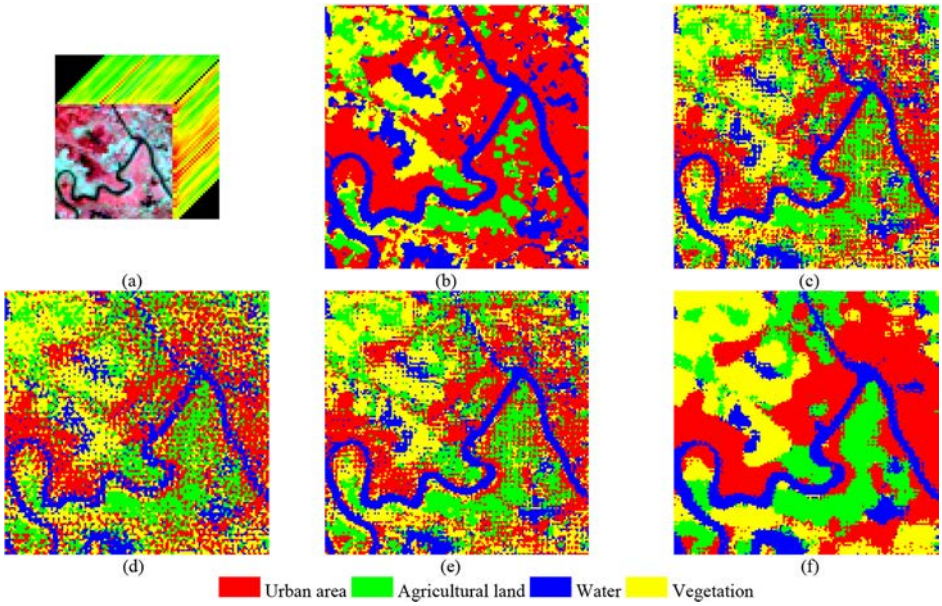

Fig. 6. Subpixel mapping results for the synthetic data set (HJ-1A). (a) Original low-resolution imagery. (b) Reference classification map obtained by eCognition software. Subpixel mapping result obtained using (c) SA, (d) GA, (e) MGA, and (f) GAAI.

method, the results of SA [see Fig. 6(c)], GA [see Fig. 6(d)], and MGA [see Fig. 6(e)] are seriously affected by the errors introduced by the spectral unmixing process, while the proposed method provides a more smooth classification map due to the correction of abundance estimation inaccuracies [see Fig. 6(f)]. However, it is obvious that some regions in the result of GAAI are over-smoothed. This is because that subpixel mapping is an inverse problem and there is a tradeoff between the refinement of abundance inaccuracies and the degree of detail preservation. As observed in Fig. 6, a generally better visual result can be obtained with the proposed method.

The subpixel mapping accuracies obtained in this experiment are listed in Table II to evaluate the effectiveness of the proposed method in quantitative fashion. As shown by Table II, the proposed GAAI provided significant improvements in terms of all quantitative indexes when compared with the SA, GA, and MGA. Specifically, a better abundance estimation can be generated with the subpixel mapping result by GAAI method. It is clear from Table II that the performance of the considered subpixel mapping methods was limited by the accuracy of the initial abundance map, but the proposed method exhibited the capacity to improve over the original abundance estimation as compared with the other three tested methods.

Moreover, the CPU time was also reported for each method in Table II. Owing to the fact that the utilized SA model is a noniterative method, this one is the fastest. However, compared with other iterative genetic algorithms-based subpixel mapping methods, the proposed method exhibits similar performance in terms of time consumption. The modified fitness function and added mutation step did not increase the computational time significantly.

2) Synthetic Image 2—Flightline C1 (FLC1): The other synthetic image used in experiments is a multispectral aerial data set containing agricultural crop species and land use, obtained in the 620–660 nm wavelengths (band number

TABLE II
ACCURACY STATISTICS FOR THE HJ-1A IMAGE EXPERIMENT

	Class	Methods			
		SA	GA	MFA	GAAI
Individual class accuracy (%)	Urban area	58.46	52.97	58.36	67.75
	Agricultural land	80.62	70.40	79.73	81.70
	Water	63.74	54.81	62.62	63.92
	Vegetation	69.04	59.88	68.37	76.19
Average class accuracy (%)		67.97	59.52	67.27%	72.39
Overall accuracy (%)		64.07	56.63	63.56	70.04
Kappa		0.505	0.403	0.498	0.580
RMSE		0.185	0.185	0.185	0.183
CPU time (s)		2.105	848.019	1988.979	811.001

12) by an optical mechanical line scanner referred to as the University of Michigan M-7 system. The flightline used in this work (called C-1) was collected on June 28, 1966 [46]. The flightline was taken over the southern part of Tippecanoe County of Indiana. It has eight land cover classes, as illustrated in Fig. 7(a) and (b). The size in pixels of the degraded low-resolution image is 20×40 pixels and the reference classification map is 80×160 pixels with a scale factor of four. Moreover, in our experiments the classification map was obtained by classifying the high-resolution image using the commercial eCognition software.

As illustrated in Fig. 7, the impact of the initial abundance map is quite important for the subsequent subpixel mapping procedure. The proposed GAAI method [see Fig. 7(f)] has a better performance on visual assessment as compared with the other three methods [see Fig. 7(c)–(e)].

Table III shows a quantitative comparison of the SA, GA, MGA, and the proposed GAAI methods. The same conclusions can be drawn as in the experiment with the HJ-1A data set. Moreover, the ability of the proposed method to generate

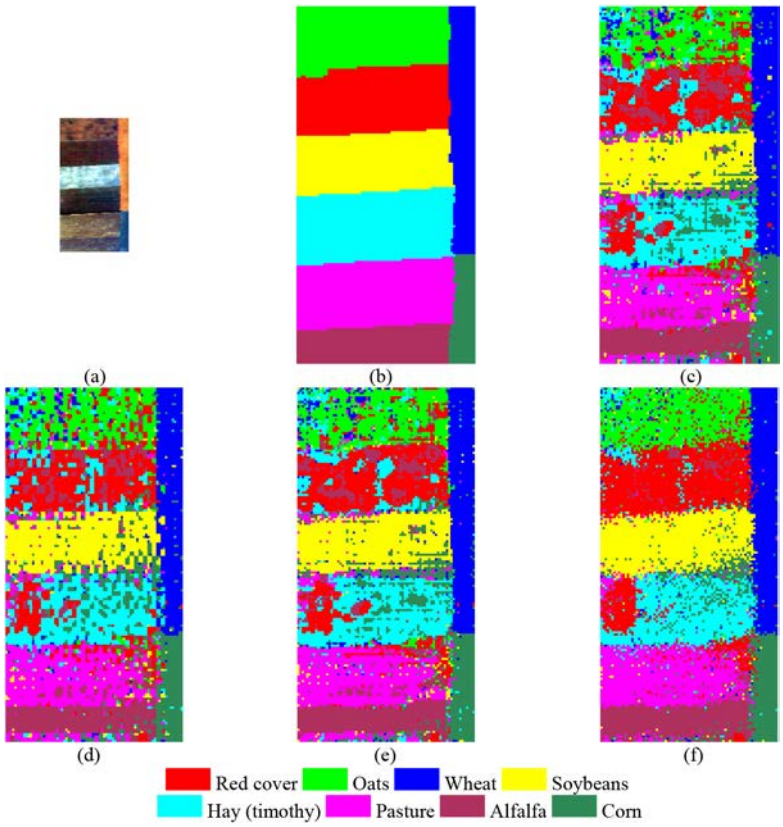

Fig. 7. Subpixel mapping results for the synthetic data set (FLC1). (a) Original low-resolution imagery. (b) Reference classification map obtained by eCognition software. Subpixel mapping result obtained using (c) SA, (d) GA, (e) MGA, and (f) GAAI.

TABLE III
ACCURACY STATISTICS FOR THE FLC1 IMAGE EXPERIMENT

	Class	Methods			
		SA	GA	MFA	GAAI
Individual class accuracy (%)	Red cover	54.94	51.14	57.68	81.35
	Oats	56.75	59.42	58.74	71.97
	Wheat	93.06	79.68	93.88	95.59
	Soybeans	79.95	75.89	80.71	86.59
	Hay (timothy)	53.03	60.22	54.87	59.73
	Pasture	64.07	70.82	64.65	70.22
	Alfalfa	71.76	66.12	72.11	84.72
	Corn	93.11	57.64	94.49	95.87
Average class accuracy (%)		70.83	65.12	72.14	80.76
Overall accuracy (%)		66.55	65.13	67.95	77.46
Kappa		0.617	0.601	0.633	0.741
RMSE		0.142	0.142	0.142	0.098
CPU time (s)		1.455	272.649	437.549	370.643

a smooth classification result is quite significant. For example, a gain of 9.51% in OA is observed for the proposed method with the FLC1 data set. Moreover, GAAI also exhibits a better RMSE result, owing to its ability to adjust the initial abundance estimations.

3) Synthetic Image 3—AVIRIS Indian Pines Dataset: The third image used in experiments is the commonly used AVIRIS Indian Pines dataset. Ten land cover classes were considered for classification. The utilized image is composed of 145×145 pixels, and the ground truth data was used as the reference data. The scale factor was set as three and Fig. 8(a) shows the degraded AVIRIS hyperspectral image cube; Fig. 8(b) shows the ground truth data in which 10 major landcover classes can be distinguished. Fig. 8(c)–(g) illustrates the subpixel mapping results using SA, GA, MGA, and the proposed methods, respectively.

As shown in Fig. 8, the impact of errors from spectral unmixing is significant, and therefore, many regions were severely misclassified. For example, the Soybeans-min class was hard to be identified owing to its spectral similarity with other classes such as Corn-notill. Therefore, all methods were affected apparently and the subpixel mapping results were limited to the spectral unmixing inaccuracies. However, it can be observed that the proposed method can still improve the final result by modifying the abundance maps.

The quantitative comparison in Table IV gives similar conclusion as the visual assessment. It is obvious that the subpixel mapping results were greatly affected by the spectral unmixing errors. If we take the Grass/Pasture class as an example, it can be seen that the individual accuracies for this class were even lower than 10%. Therefore, the subpixel mapping results for this image are not as satisfactory as for the other data sets tested owing to the difficulty of spectral unmixing for this particular scene, in which spectra of different classes were very similar to each other. However, it can also be concluded from our experiment that the proposed method can improve the subpixel mapping performance by incorporating the abundance map accuracies.

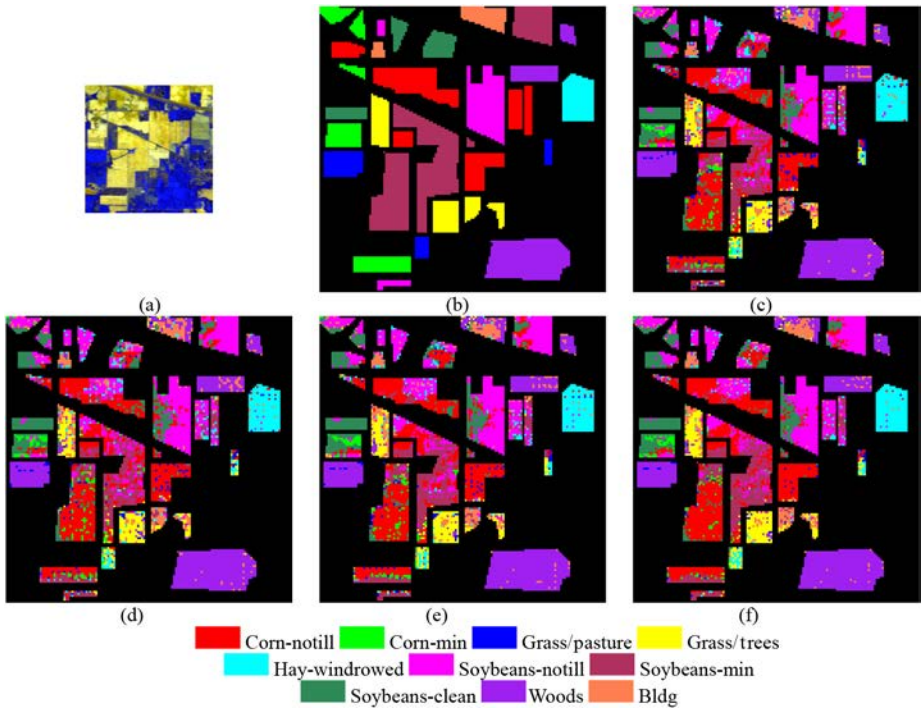

Fig. 8. Subpixel mapping results for the synthetic data set (AVIRIS). (a) Original low-resolution imagery. (b) The ground truth data as the reference classification map. Subpixel mapping result obtained using (c) SA, (d) GA, (e) MGA, and (f) GAAI.

TABLE IV
ACCURACY STATISTICS FOR THE AVIRIS IMAGE EXPERIMENT

	Class	Methods			
		SA	GA	MFA	GAAI
Individual class accuracy (%)	Corn-notill	44.00	44.34	45.78	49.24
	Corn-min	12.52	12.67	12.22	10.86
	Grass/Pasture	6.79	6.53	5.74	4.70
	Grass/Trees	52.87	49.04	53.91	58.09
	Hay-windrowed	92.70	91.57	94.10	96.91
	Soybeans-notill	61.86	61.71	62.15	62.89
	Soybeans-min	25.58	25.03	26.51	28.64
	Soybeans-clean	39.56	40.05	39.56	41.52
	Woods	94.78	94.10	95.07	96.52
	Bldg	48.68	49.43	48.30	53.21
Average class accuracy (%)		47.93	47.44	48.33	50.26
Overall accuracy (%)		46.41	45.92	47.04	48.97
Kappa		0.391	0.386	0.398	0.419
RMSE		0.080	0.080	0.080	0.077
CPU time (s)		2.432	965.346	2143.534	840.286

B. Result Experiments—Nuance Data Set

Our real experiments were conducted using a pair of low- and high-spatial resolution images collected simultaneously over the same area. The low-spatial resolution image (of size 50×50 pixels) was collected using the Nuance NIR imaging spectrometer [see Fig. 9(a)]. The acquired image has 46 bands, collected in the spectral range from 650 to 1100 nm and with 10 nm spectral sampling interval. The high-spatial resolution color image (of size 150×150 pixels) was obtained by a digital camera for the same area [see Fig. 9(b)], and the scale factor was exactly three with regards to the low-spatial resolution hyperspectral image. Three major landcover classes can be distinguished in this scene: withered vegetation, fresh vegetation, and black paper, used as the background. A reference classification map was obtained by using the SVM technique on the high-spatial resolution color image, which gave the result reported on Fig. 9(c). The subpixel mapping results (obtained with different methods) are reported on Fig. 9(d)–(g).

As shown in Fig. 9, the proposed method can provide a better visual result. However, some important details may also be removed due to unmixing errors and excessive smoothing as mentioned before. This kind of tradeoff between smoothing and detail preservation is inevitable for subpixel mapping.

As illustrated in Table V, the proposed GAAI also provided improvements in this experiment in terms of all indexes when compared with the SA, GA, and MGA. The RMSE index also showed improvements. Unlike the synthetic experiments, additional error sources were introduced in the real experiment such as the registration error between the low-resolution hyperspectral image and the high-resolution color image. However, GAAI method still was able to obtain the highest accuracy under the same circumstances.

C. Parameter Analysis

1) Impact of the Weighted Parameter λ: In this section, we evaluate the impact of parameter λ on the accuracy of the proposed GAAI method. Fig. 10 shows the OA as a function of different values of this parameter for two of the considered

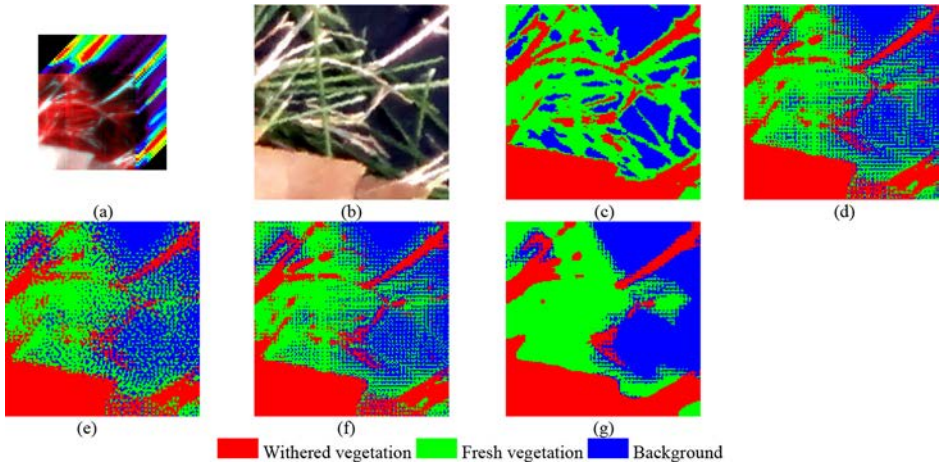

Fig. 9. Subpixel mapping results for the real experiment. (a) Low-spatial resolution image obtained by the Nuance NIR imaging spectrometer. (b) High-spatial resolution color image obtained by a high-resolution digital camera. (c) Reference classification result obtained by the SVM. Subpixel mapping results obtained by (d) SA, (e) GA, (f) MGA, and (g) GAAI.

TABLE V
ACCURACY STATISTICS FOR THE NUANCE IMAGE EXPERIMENT

Class		Methods			
		SA	GA	MFA	GAAI
Individual class accuracy (%)	Urban area	84.75	81.04	84.50	86.62
	Agricultural land	61.72	59.74	61.64	66.58
	Water	66.73	64.62	66.51	73.31
Average class accuracy (%)		71.07	68.47	70.88	75.50
Overall accuracy (%)		69.95	67.42	69.78	74.38
Kappa		0.545	0.507	0.542	0.612
RMSE		0.196	0.196	0.196	0.189
CPU time (s)		1.572	617.307	1633.60	614.831

hyperspectral scenes (HJ-1A and Nuance data sets). As shown in Fig. 10, the curves for both images exhibit a similar shape.

Generally speaking, small values of parameter λ result in stable OAs and the optimal parameter value is around two for the proposed GAAI method. As λ increases greatly, the OA scores decrease and become less stable. However, a better result can be obtained for most parameter values compared with the other three traditional methods.

2) Impact of Combination of Fitness Function and Operators: In this section, we evaluate the utilization of the mutation operator and the weighted spectral term. To verify the effectiveness of the two modifications in the proposed GAAI method, different combinations of the fitness function and operators were tested for both images (HJ-1A and Nuance data sets) as Fig. 11 depicts.

Apparently, both the mutation operator and the spectral term contribute to the performance of the GAAI method greatly. Although the mutation operator can lead to greater improvements as compared with the spectral term, it is essential to introduce the spectral term to retain the consistency between the original hyperspectral imagery and the generated subpixel mapping result.

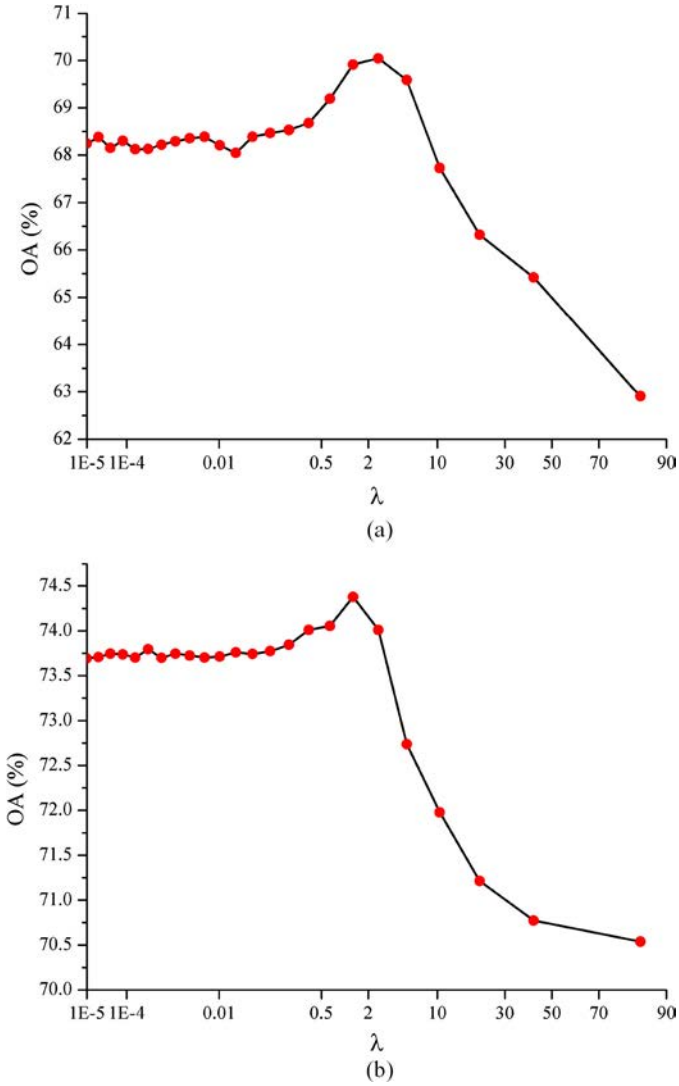

Fig. 10. Impact of parameter λ on the classification accuracy obtained by the proposed GAAI method. (a) Synthetic image experiment (HJ-1A). (b) Real image experiment (Nuance).

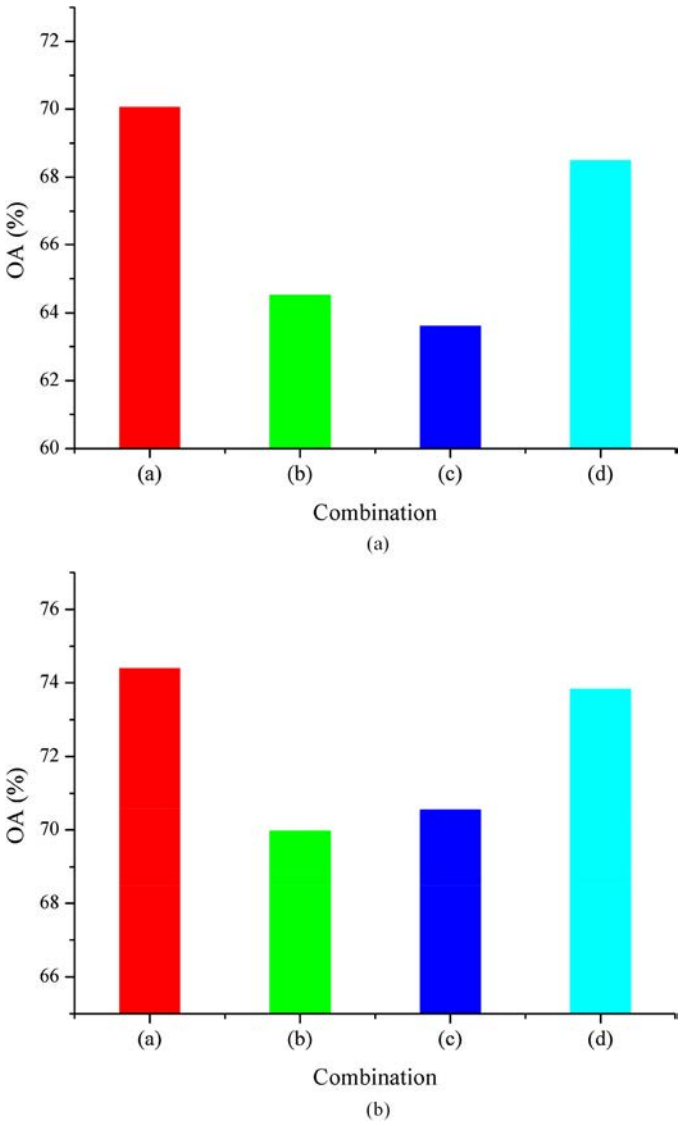

Fig. 11. Impact of using different fitness functions and operators on the classification accuracy. (a) Synthetic image experiment (HJ-1A). (b) Real image experiment (Nuance). (a) Proposed GAAI method. (b) Fitness (GAAI) + Operator (GA). (c) Fitness (GAAI) + Operator (MGA). (d) Fitness (SD) + Operator (GAAI).

IV. Conclusion and Future Research Lines

This paper has introduced a novel subpixel mapping method based on genetic algorithms which has the potential to correct possible errors in the initial abundance estimations by means of a mutation operator. As a result, a new feature of our proposed approach is that it can correct possibly inaccurate abundance estimations used as the initial condition in the subpixel mapping process. In this regard, a major difference of the proposed approach with regards to other traditional subpixel mapping methods is that we do not assume that the initial abundance map is completely accurate, but instead use a mutation operator to adjust the attribution of subpixels in order to refine the final mapping result. Moreover, our method incorporates a weighted spectral term into the fitness function that is combined with the spatial term commonly adopted by other methods. Our experimental results, conducted using both synthetic and real hyperspectral images, indicate that our method provides comparable or better results than those obtained by other three traditional subpixel mapping algorithms. A detailed parameter analysis also shows that both the mutation operator and the weighted spectral term introduced by our proposed method play significant key roles in obtaining a better subpixel mapping result.

Another important observation is that the proposed method can only adjust the abundance map and the final subpixel mapping result slightly, and therefore, unmixing may still contribute significantly to the final subpixel mapping results. Future research will focus on conducting additional experiments with other data sets, designing strategies for adaptively setting the input parameter λ, and testing the impact of different kinds of spectral unmixing techniques in the task of generating the initial abundance map used for subpixel mapping purposes.

Acknowledgment

The authors appreciate greatly the valuable comments and suggestions of the anonymous reviewers for improving the paper.

References

[1] J. M. Bioucas-Dias, A. Plaza, G. Camps-Valls, P. Scheunders, N. M. Nasrabadi, and J. Chanussot, "Hyperspectral remote sensing data analysis and future challenges," *IEEE Geosci. Remote Sens. Mag.*, vol. 1, no. 2, pp. 6–36, Jun. 2013.

[2] P. M. Atkinson, "Mapping sub-pixel boundaries from remotely sensed images," in *Innovations in GIS IV*. London, U.K.: Taylor & Francis, 1997, ch. 12, pp. 166–180.

[3] P. M. Atkinson, "Issues of uncertainty in super-resolution mapping and their implications for the design of an inter-comparison study," *Int. J. Remote Sens.*, vol. 30, no. 20, pp. 5293–5308, 2009.

[4] K. C. Mertens, L. P. C. Verbeke, and R. R. D. Wulf, "Sub-pixel mapping with neural networks: Real-world spatial configurations learned from artificial shapes," in *Proc. 4th Int. Symp. Remote Sens.*, Jun. 2003, pp. 1–5.

[5] K. C. Mertens, L. P. C. Verbeke, T. Westra, and R. R. D. Wulf, "Sub-pixel mapping and sub-pixel sharpening using neural network predicted wavelet coefficients," *Remote Sens. Environ.*, vol. 91, no. 2, pp. 225–236, May 2004.

[6] A. J. Tatem, H. G. Lewis, P. M. Atkinson, and M. S. Nixon, "Super-resolution target identification from remotely sensed images using a Hopfield neural network," *IEEE Trans. Geosci. Remote Sens.*, vol. 39, no. 4, pp. 781–796, Apr. 2001.

[7] A. J. Tatem, H. G. Lewis, P. M. Atkinson, and M. S. Nixon, "Increasing the spatial resolution of agricultural land cover maps using a Hopfield neural network," *Int. J. Geog. Inf. Sci.*, vol. 17, no. 7, pp. 647–672, 2003.

[8] X. Xu, Y. Zhong, and L. Zhang, "Adaptive sub-pixel mapping based on a multi-agent system for remote sensing imagery," *IEEE Trans. Geosci. Remote Sens.*, vol. 52, no. 2, pp. 787–804, Feb. 2014.

[9] K. C. Mertens, L. P. C. Verbeke, E. I. Ducheyne, and R. R. De Wulf, "Using genetic algorithms in sub-pixel mapping," *Int. J. Remote Sens.*, vol. 24, no. 21, pp. 4241–4247, Nov. 2003.

[10] A. Villa, J. Chanussot, J. A. Benediktsson, and C. Jutten, "Spectral unmixing for the classification of hyperspectral images at a finer spatial resolution," *IEEE J. Sel. Topics Signal Process.*, vol. 5, no. 3, pp. 521–533, Jun. 2011.

[11] J. Verhoeye and R. De Wulf, "Land cover mapping at sub-pixel scales using linear optimization techniques," *Remote Sens. Environ.*, vol. 79, no. 1, pp. 96–104, Jan. 2002.

[12] Y. Zhong and L. Zhang, "Remote sensing image sub-pixel mapping based on adaptive differential evolution," *IEEE Trans. Syst. Man Cybern. B Cybern.*, vol. 42, no. 5, pp. 1306–1329, Oct. 2012.

[13] Y. Zhong and L. Zhang, "Sub-pixel mapping based on artificial immune systems for remote sensing imagery," *Pattern Recog.*, vol. 46, no. 11, pp. 2902–2926, Nov. 2013.

[14] Q. Wang, L. Wang, and D. Liu, "Particle swarm optimization-based sub-pixel mapping for remote-sensing imagery," *Int. J. Remote Sens.*, vol. 33, no. 20, pp. 6480–6496, 2012.
[15] K. C. Mertens, B. De Baets, L. P. C. Verbeke, and R. R. De Wulf, "A sub-pixel mapping algorithm based on sub-pixel/pixel spatial attraction models," *Int. J. Remote Sens.*, vol. 27, no. 15, pp. 3293–3310, Aug. 2006.
[16] P. M. Atkinson, "Sub-pixel target mapping from soft-classified remotely sensed imagery," *Photogramm. Eng. Remote Sens.*, vol. 71, no. 7, pp. 839–846, Jul. 2005.
[17] T. Kasetkasem, M. K. Arora, and P. K. Varshney, "Super-resolution land cover mapping using a Markov random field based approach," *Remote Sens. Environ.*, vol. 96, no. 3/4, pp. 302–314, Jun. 2005.
[18] X. Xu, Y. Zhong, L. Zhang, and H. Zhang, "Sub-pixel mapping based on a MAP model with multiple shifted hyperspectral imagery," *IEEE J. Sel. Topics Appl. Earth Observ. Remote Sens.*, vol. 6, no. 2, pp. 580–593, Apr. 2013.
[19] M. W. Thornton, P. M. Atkinson, and D. A. Holland, "A linearised pixel swapping method for mapping rural linear land cover features from spatial resolution remotely sensed imagery," *Comput. Geosci.*, vol. 33, no. 10, pp. 1261–1272, Oct. 2007.
[20] A. Boucher, P. C. Kyriakidis, and C. Cronkite-Ratcliff, "Geostatistical solutions for super-resolution land cover mapping," *IEEE Trans. Geosci. Remote Sens.*, vol. 46, no. 1, pp. 272–283, Jan. 2008.
[21] Q. Wang and W. Shi, "Utilizing multiple subpixel shifted images in sub-pixel mapping with image interpolation," *IEEE Geosci. Remote Sens. Lett.*, vol. 11, no. 4, pp. 798–802, Apr. 2013.
[22] Q. Wang, W. Shi, and P. M. Atkinson, "Sub-pixel mapping of remote sensing images based on radial basis function interpolation," *ISPRS J. Photogramm. Remote Sens.*, vol. 92, pp. 1–15, Jun. 2014.
[23] Y. Ge, Y. Chen, S. Li, and Y. Jiang, "Vectorial boundary-based sub-pixel mapping method for remote-sensing imagery," *Int. J. Remote Sens.*, vol. 35, no. 5, pp. 1756–1768, 2014.
[24] Y. Ge, S. Li, and V. C. Lakhan, "Development and testing of a subpixel mapping algorithm," *IEEE Trans. Geosci. Remote Sens.*, vol. 47, no. 7, pp. 2155–2164, Jul. 2009.
[25] T. Kasetkasem, M. K. Arora, and P. K. Varshney, "Super-resolution land cover mapping using a Markov random field based approach," *Remote Sens. Environ.*, vol. 96, no. 3/4, pp. 302–314, Jun. 2005.
[26] H. J. Huang, J. Yu, and W. D. Sun, "Superresolution mapping using multiple dictionaries by sparse representation," *IEEE Geosci. Remote Sens. Lett.*, vol. 11, no. 12, pp. 2055–2059, Dec. 2014.
[27] F. Ling *et al.*, "Post-processing of interpolation-based super-resolution mapping with morphological filtering and fraction refilling," *Int. J. Remote Sens.*, vol. 35, no. 13, pp. 5251–5262, 2014.
[28] Y. F. Su, G. M. Foody, A. M. Muad, and K. S. Cheng, "Combining pixel swapping and contouring methods to enhance super-resolution mapping," *IEEE J. Sel. Topics Appl. Earth Observ. Remote Sens.*, vol. 5, no. 5, pp. 1428–1437, Oct. 2012.
[29] Y. F. Zhong, Y. Y. Wu, X. Xu, and L. P. Zhang, "An adaptive subpixel mapping method based on MAP model and class determination strategy for hyperspectral remote sensing imagery," *IEEE Trans. Geosci. Remote Sens.*, vol. 53, no. 3, pp. 1411–1426, Mar. 2015.
[30] C. H. Zhao, W. Liu, Y. L. Wang, and X. H. Li, "Modified genetic algorithm-based sub-pixel mapping," *Int. J. Light Electron Opt.*, vol. 125, no. 21, pp. 6379–6383, Nov. 2014.
[31] L. Li, Y. Chen, T. Xu, R. Liu, K. Shi, and C. Huang, "Super-resolution mapping of wetland inundation from remote sensing imagery based on integration of back-propagation neural network and genetic algorithm," *Remote Sens. Environ.*, vol. 164, no. 3/4, pp. 142–154, Jul. 2015.
[32] U. Maulik and S. Bandyopadhyar, "Genetic algorithm-based clustering technique," *Pattern Recog.*, vol. 33, no. 9, pp. 1455–1465, Sep. 2000.
[33] K. Tang, K. Man, S. Kwong, and Q. He, "Genetic algorithms and their applications," *IEEE Signal Process. Mag.*, vol. 13, no. 6, pp. 22–37, Nov. 1996.
[34] T. Celik, "Change detection in satellite images using a genetic algorithm approach," *IEEE Geosci. Remote Sens. Lett.*, vol. 7, no. 2, pp. 386–390, Apr. 2010.
[35] J. Senthilnath, X-S. Yang, and J. A. Benediktsson, "Automatic registration of multi-temporal remote sensing images based on nature inspired techniques," *Int. J. Image Data Fusion*, vol. 5, no. 4, pp. 263–284, 2014.
[36] M. Srinivas and L. Patnaik, "Genetic algorithms: A survey," *Computer*, vol. 27, no. 6, pp. 17–26, Jun. 1994.
[37] D. Chang, X. Zhang, and C. Zheng, "A genetic algorithm with gene rearrangement for K-means clustering," *Pattern Recog.*, vol. 42, no. 7, pp. 1210–1222, Jul. 2009.
[38] J. Senthilnath, N. P. Kalro, and J. A. Benediktsson, "Accurate point matching based on multi-objective genetic algorithm for multi-sensor satellite imagery," *Appl. Math. Comput.*, vol. 236, pp. 546–564, 2014.
[39] X. Xu, "Sub-pixel mapping theory considering spatial characteristic for remote sensing imagery," Ph.D. dissertation, LIESMARS, Wuhan Univ., Wuhan, China, 2013.
[40] J. M. Bioucas-Dias *et al.*, "Hyperspectral unmixing overview: Geometrical, statistical and sparse regression-based approaches," *IEEE J. Sel. Topics Appl. Earth Observ. Remote Sens.*, vol. 5, no. 2, pp. 354–379, Apr. 2012.
[41] W. R. Tobler, "A computer movie simulating urban growth in the Detroit region," *Econ. Geogr.*, vol. 46, pp. 234–240, Jun. 1970.
[42] X. Li, C. Cao, and C. Chang, "The first law of geography and spatial temporal proximity," *Chin. J. Nat.*, vol. 29, no. 2, pp. 69–71, 2007.
[43] D. Heinz and C.-I. Chang, "Fully constrained least squares linear spectral mixture analysis method for material quantification in hyperspectral imagery," *IEEE Trans. Geosci. Remote Sens.*, vol. 39, no. 3, pp. 529–545, Mar. 2001.
[44] J. Senthilnath, D. Kumar, J. A. Benediktsson, and X. Zhang, "A novel hierarchical clustering technique based on splitting and merging" *Int. J. Image Data Fusion*, vol. 34, no. 23, pp. 543–567, 2015.
[45] G. X. Bai, "China environmental and disaster monitoring and forecasting small satellite —HJ-1A/B," *Aerosp. China*, vol. 5, pp. 10–15, 2009.
[46] R. M. Hoffer, "Computer-aided analysis of multispectral scanner data-the beginnings," in *Proc. ASPRS 2009 Annu. Conf.*, Mar. 9-13, 2009.

Xiaohua Tong received the Ph.D. degree in Transportation Planning and Management from Tongji University, Shanghai, China, in 1999.

He worked as a Postdoctoral Researcher with the State Key Laboratory of Information Engineering in Surveying, Mapping, and Remote Sensing, Wuhan University, Wuhan, China, between 2001 and 2003; he was a Research Fellow with The Hong Kong Polytechnic University, in 2006, Hung Hom, Hong Kong, and a Visiting Scholar at the University of California, Santa Barbara, CA, USA, between 2008 and 2009. He is also a "Chang-Jiang Scholar" Chair Professor appointed by the Ministry of Education, China. His research interests include remote sensing, GIS, trust in spatial data, image processing for high-resolution, and hyperspectral images.

Dr. Tong serves as the Vice-Chair of the Commission on Spatial Data Quality of the International Cartographical Association, and the Co-Chair of the ISPRS working group (WG II/4) on Spatial Statistics and Uncertainty Modeling.

Xiong Xu received the B.Sc. degree in photogrammetry, and the Ph.D. degree in photogrammetry and remote sensing, from Wuhan University, Wuhan, China, in 2008 and 2013, respectively.

Currently, he is a Research Assistant with the College of Surveying and Geoinformatics, Tongji University, Shanghai, China. His research interests include multi- and hyperspectral image processing, artificial neural network, and pattern recognition.

Antonio Plaza (M'05–SM'07–F'15) received the degree in computer engineering, and the M.Sc. and Ph.D. degrees in computer engineering from the University of Extremadura, Badajoz, Spain, in 1998, 2000, and 2002, respectively.

He is an Associate Professor (with accreditation for Full Professor) with the Department of Technology of Computers and Communications, University of Extremadura, Badajoz, Spain, where he is the Head of the Hyperspectral Computing Laboratory (HyperComp). He was the Coordinator of the Hyperspectral Imaging Network, a European project with total funding of 2.8 MEuro, from 2007 to 2011. He has authored more than 500 publications, including more than 150 JCR journal papers (106 in IEEE journals), 22 book chapters, and over 250 peer-reviewed conference proceeding papers (125 in IEEE conferences). He has guest-edited seven special issues on JCR journals (three in IEEE journals).

Prof. Plaza has been a Chair for the IEEE Workshop on Hyperspectral Image and Signal Processing: Evolution in Remote Sensing, in 2011 and also an Associate Editor for the *IEEE Geoscience and Remote Sensing Magazine*, and was a Member of the Editorial Board of the IEEE Geoscience and Remote Sensing Newsletter from 2011 to 2012, and a Member of the Steering Committee of the IEEE JOURNAL OF SELECTED TOPICS IN APPLIED EARTH OBSERVATIONS AND REMOTE SENSING in 2012. He served as the Director of Education Activities for the IEEE Geoscience and Remote Sensing Society (GRSS) from 2011 to 2012, and has been serving as the President of the Spanish Chapter of the IEEE GRSS since November 2012. Since January 2013, he has been serving as the Editor-in-Chief for the IEEE TRANSACTIONS ON GEOSCIENCE AND REMOTE SENSING Journal. He was a recipient of the recognition of Best Reviewers of the IEEE TRANSACTIONS ON GEOSCIENCE AND REMOTE SENSING LETTERS, in 2009, and also a recipient of the recognition of Best Reviewers of the IEEE TRANSACTIONS ON GEOSCIENCE AND REMOTE SENSING, in 2010, a journal for which he has served as Associate Editor from 2007 to 2012.

Huan Xie received the B.S. degree in surveying engineering, and the M.S. and Ph.D. degrees in cartography and geoinformation from Tongji University, Shanghai, China, in 2003, 2006, and 2009, respectively.

From 2007 to 2008, she was with the Institute of Photogrammetry and GeoInformation, Leibniz Universität Hannover, Hannover, Germany, funded by China Scholarship Council, as a Visiting Scholar. Since June 2009, she has been with the College of Surveying and Geoinformatics, Tongji University, where she is currently an Associate Professor and teaches courses related to GIS and remote sensing. Her research interests include hyperspectral remote sensing and polar remote sensing.

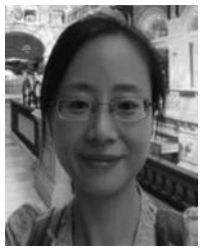

Haiyan Pan received the B.Sc. degree in surveying engineering and the M.S. degree in geographical information system from East China Institute of Technology, Nanchang, China, in 2004 and 2007, respectively. Currently, she is pursuing the Ph.D. degree in cartography and geographical information engineering at the College of Surveying and Geoinformatics, Tongji University, Shanghai, China.

Her research interests include hyperspectral change detection and data analysis.

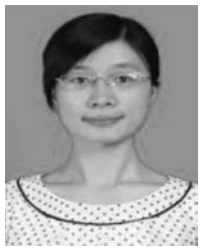

Wen Cao received the M.S. degree in photogrammetry and remote sensing from China University of Mining and Technology, Xuzhou, China. Currently, she is pursuing the Ph.D. degree in cartography and geographical information engineering at the College of Surveying and Geoinformatics at Tongji University, Shanghai, China.

Her research interests include multisource remote sensing data processing and feature recognition.

Dong Lv, photograph and biography not available at the time of publication